

## Supporting information for

### Higher apparent gas transfer velocities for CO<sub>2</sub> compared to CH<sub>4</sub> in small lakes

Gustav Pajala<sup>a\*</sup>, David Rudberg<sup>a</sup>, Magnus Gålfalk<sup>a</sup>, John Michael Melack<sup>b,c</sup>, Sally Macintyre<sup>b,c,d</sup>, Jan Karlsson<sup>e</sup>, Henrique Oliveira Sawakuchi<sup>a</sup>, Jonathan Schenk<sup>a</sup>, Anna Sieczko<sup>a</sup>, Ingrid Sundgren<sup>a</sup>, Nguyen Thanh Duc<sup>a</sup>, David Bastviken<sup>a\*</sup>

<sup>a</sup>Department of Thematic Studies – Environmental Change, Linköping University, 58183 Linköping, Sweden.

<sup>b</sup>Department of Ecology, Evolution and Marine Biology, University of California, Santa Barbara, California, USA

<sup>c</sup>Earth Research Institute, University of California, Santa Barbara, California, USA

<sup>d</sup>Marine Science Institute, University of California, Santa Barbara, California, USA

<sup>e</sup>Climate Impacts Research Centre, Department of Ecology and Environmental Sciences - Umeå University, Umeå, Sweden

\*Corresponding authors at: Department of Thematic Studies – Environmental Change, Linköping University, 58183 Linköping, Sweden.

\*E-mail address: [Gustav.pajala@liu.se](mailto:Gustav.pajala@liu.se) and [david.bastviken@liu.se](mailto:david.bastviken@liu.se)

## **Contents**

**Text S1.** Calculation of gas fluxes in SOR, BOL, and SOD.

**Text S2.** Calculation of microbubble flux contribution.

**Figure S1.** Relationship between CO<sub>2</sub> and CH<sub>4</sub> water concentrations (panel a) and gas fluxes (panel b).

**Figure S2.** Relationship between the  $k_{600}$  ratio for CO<sub>2</sub> and CH<sub>4</sub> versus CO<sub>2</sub> saturation (panel a) and CH<sub>4</sub> saturation (panel b).

**Figure S3.** CO<sub>2</sub> and CH<sub>4</sub> gas measurement over time using the Ultra-Portable Greenhouse-gas analyzer (UGGA).

**Figure S4.** Fieldwork setup using a flux chamber (FC) connected to the UGGA for gas measurements.

**Number of figures: 4**

**Number of equations: 2**

**Number of pages: 9**

1 **Text S1** (calculation of gas fluxes in SOR, BOL, and SOD)

2 Linear regressions for calculating the gas accumulation rates for CO<sub>2</sub> and CH<sub>4</sub>, representing  
3 the increase in mole fraction per time unit (ppm d<sup>-1</sup>), were made in Excel using the function  
4 SLOPE for time periods of 40 to 100 seconds.  $R^2$  values for the linear regressions were  
5 determined using the function RSQ where linear regressions having and  $R^2 > 0.7$  were used as  
6 final gas accumulation rates. To convert gas accumulation rates to gas fluxes  $F_{\text{gas}}$  (mmol m<sup>-2</sup>  
7 d<sup>-1</sup>), we applied the ideal gas law and divided with the chamber area, see Equation (S1),

$$8 \quad F_{\text{gas}} = \frac{\text{ppm}}{t} * \frac{(PV*0.0001)}{RTA} \quad (\text{S1})$$

9 where the barometric pressure  $P$  (hPa) was obtained from the Swedish Meteorological and  
10 Hydrological Institute (SMHI) MESAN model,  $V$  represents the chamber headspace volume  
11 (m<sup>3</sup>), 0.0001 was as used as a conversion factor to convert the gas accumulation rates (ppm d<sup>-1</sup>  
12 <sup>1</sup>) and the barometric pressure (hPa) to (pa d<sup>-1</sup>),  $R$  is the ideal gas constant, 8.314 (m<sup>3</sup> Pa K<sup>-1</sup>  
13 mol<sup>-1</sup>),  $T$  represents the water temperature (K), and  $A$  represents the chamber area (m<sup>2</sup>).

14

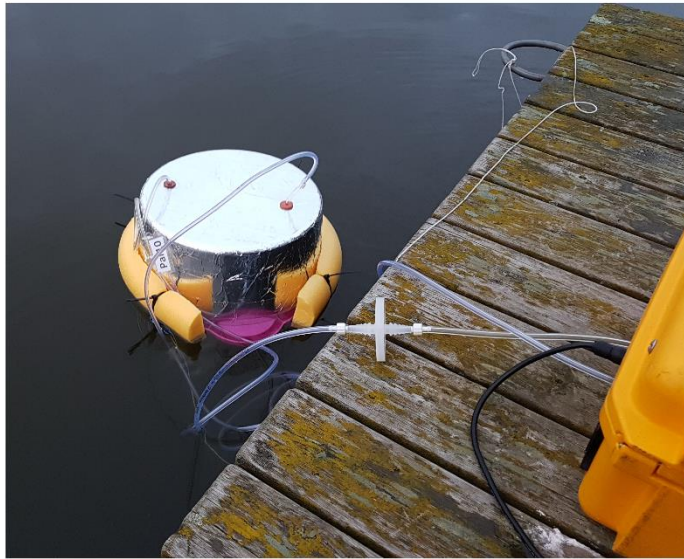
15 **Text S2** (calculation of microbubble flux)

16 Microbubble mediated flux  $F_{mb}$  ( $\text{mol m}^{-2} \text{d}^{-1}$ ) was calculated based on the equation from  
17 Prairie & Del Giorgio<sup>1</sup>, using the apparent  $k_{600}$  calculated for  $\text{CO}_2$  corrected to  $\text{CH}_4$ , according  
18 to equation (S2) below:

$$19 \quad F_{mb} = F_{\text{CH}_4} - k_{600\text{CO}_2} * kH [p_{\text{CH}_4\text{water}} - p_{\text{CH}_4\text{air}}] \quad (\text{S2})$$

20 where  $F_{\text{CH}_4}$  is the observed  $\text{CH}_4$  flux ( $\text{mol m}^{-2} \text{d}^{-1}$ ),  $k_{600\text{CO}_2}$  is the apparent  $k_{600}$  for  $\text{CO}_2$   
21 normalized to a Schmidt number of 600 ( $\text{m d}^{-1}$ ),  $kH$  is the temperature corrected Henry's law  
22 constant ( $\text{M atm}^{-1}$ ),  $p_{\text{CH}_4\text{water}}$  is the partial pressure of  $\text{CH}_4$  in equilibrium with the surface  
23 water concentration (atm) and  $p_{\text{CH}_4\text{air}}$  is the partial pressure in the flux chamber at sampling  
24 (atm).

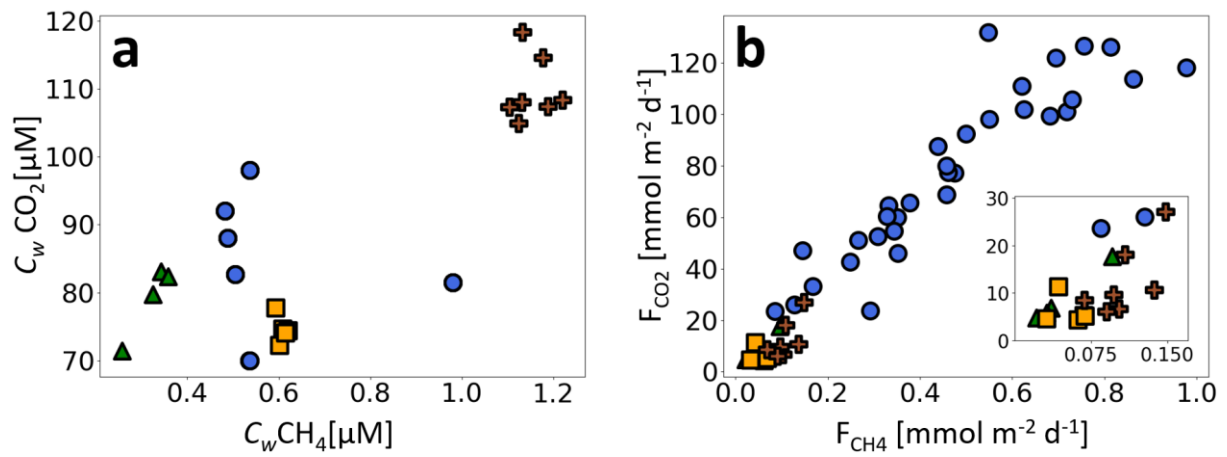
25



26

27 **Figure S1.** Gas sampling setup using the UGGA in SOR, BOL, and SOD (photo by G. Pajala).

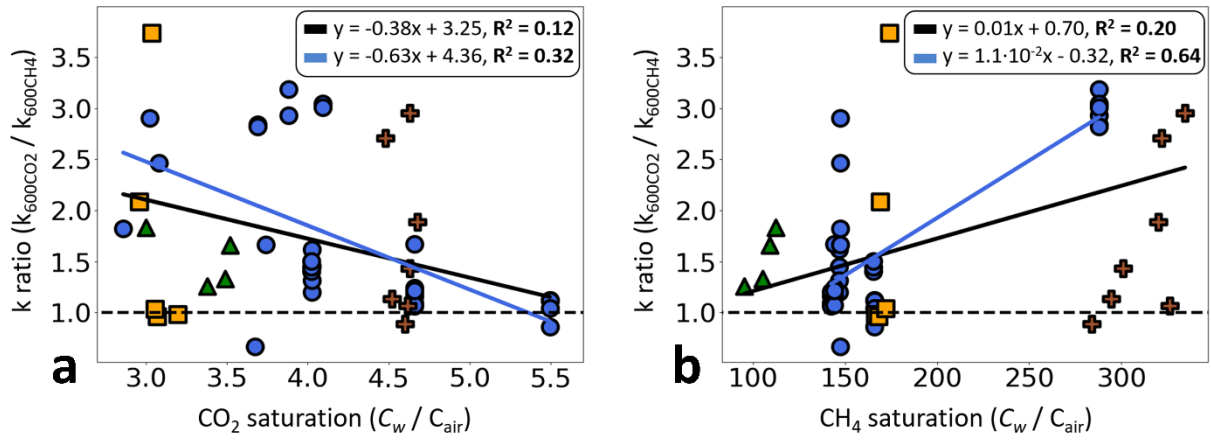
28



29

30 **Figure S2.** Relations between (a) surface water concentrations of CH<sub>4</sub> and CO<sub>2</sub> ( $C_w \text{CH}_4$  and  $C_w \text{CO}_2$ ) and (b) diffusive  
 31 fluxes of CH<sub>4</sub> and CO<sub>2</sub>. Lake observations are represented by blue circles (OBJ), green triangles (BOL), orange  
 32 squares (SOD) and brown crosses (SOR). The inset graph in panel B shows a zoom of the low flux observations.

33



34

35 **Figure S3.** Relation between  $k_{600\text{CO}_2}/k_{600\text{CH}_4}$  ratio and **(a)**  $\text{CO}_2$  saturation and **(b)**  $\text{CH}_4$  saturation. Lake observations  
 36 are represented by blue circles (OBJ), green triangles (BOL), orange squares (SOD) and brown crosses (SOR).  
 37 Regressions are calculated for all lakes combined (black line) and for OBJ (blue line). The dashed line denotes the  
 38 separation between higher (above) and lower (below)  $k_{600\text{CO}_2}$  than  $k_{600\text{CH}_4}$ .



39

40

41 **Figure S4.** Screenshot from continuous CH<sub>4</sub> (top) and CO<sub>2</sub> (bottom) measurement in a gas equilibrator used in  
 42 aquatic environments, showing differences in equilibration time among gases. In this equilibrator, CO<sub>2</sub>  
 43 equilibrium was reached after approximately 8 minutes, whereas CH<sub>4</sub> still changed linearly after 20 minutes  
 44 without any sign of approaching equilibrium (photo by D. Bastviken).

45

46



47   References

48

- 49   1.       Prairie, Y.; del Giorgio, P., A new pathway of freshwater methane emissions and the putative  
50   importance of microbubbles. *Inland Waters* **2013**, 3 (3), 311-320.

51